Simulations of nanoscale interferometer and array focusing by metal heterowaveguides

Bing Wang and Guo Ping Wang

Department of Physics, Wuhan University, Wuhan 430072, China

kp_wang@hotmail.com

Abstract: We propose a three-dimensional (3D) nanoscale metal heterowaveguide for nanoguiding of light in nanometric cross section. Finite-difference time-domain simulation reveals that a light beam with 35nm×55nm cross section can effectively propagate along the heterowaveguides with 2.84dB/μm energy loss. 3D nanoscale Mach-Zehnder interferometers and metal waveguide arrays constructed by such heterowaveguides show interesting sensing and array nanofocusing properties, implying potential applications in the fields of nanophotonics such as nanosensing, nanolithography, array imaging, and controlling of the flow of light etc.

OCIS codes: (240.6680) Surface plasmons; (230.3120) Integrated optics devices; (040.1240) Arrays; (220.2560) Focus.

References and links

1. J. R. Krenn, J. C. Weeber, A. Dereux, E. Bourillot, J. P. Goudonnet, B. Schider, A. Leitner, F. R. Aussenegg, and C. Girard, "Direct observation of localized surface plasmon coupling," Phys. Rev. B **60**, 5029-5033 (1999).
2. S. A. Maier, P. G. Kik, H. A. Atwater, S. Meltzer, E. Harel, B. E. Koel, and A. A. G. Requicha, "Local detection of electromagnetic energy transport below the diffraction limit in metal nanoparticle plasmon waveguides," Nature Mater. **2**, 229-232 (2003).
3. B. Wang and G. P. Wang, "Surface plasmon polariton propagation in nanoscale metal gap waveguides," Opt. Lett. **29**, 1992-1994 (2004).
4. K. Tanaka and M. Tanaka, "Simulations of nanometric optical circuits based on surface plasmon polariton gap waveguide," Appl. Phys. Lett. **82**, 1158-1160 (2003).
5. K. Tanaka, M. Tanaka, and T. Sugiyama, "Simulations of partical nanometric optical circuits based on surface plasmon polariton gap waveguide," Opt. Express **13**, 256-266 (2005).
6. B. Wang and G. P. Wang, "Metal heterowaveguides for nanometric focusing of light," Appl. Phys. Lett. **85**, 3599-3601 (2004).
7. B. Wang and G. P. Wang, "Directional beaming of light from a nanoslit surrounded by metallic heterostructures," Appl. Phys. Lett. (to be published).
8. B. Wang and G. P. Wang, "Plasmon Bragg reflectors and nanocavities on flat metallic surfaces," Appl. Phys. Lett. **87**, 013107 (2005).
9. K. S. Yee, "Numerical solution of initial boundary value problems involving Maxwell equations in isotropic media," IEEE Trans. Antennas Propagat. **AP-14**, 302-307 (1966).
10. E. D. Palik, *Handbook of optical constants of solids* (Academic, New York, 1985).
11. Z. Y. Li and K. M. Ho, "Anomalous propagation loss in photonic crystal waveguides," Phys. Rev. Lett. **92**, 063904 (2004).
12. N. S. Stoyanov, D. W. Ward, T. Feurer, and K. A. Nelson, "Terahertz polariton propagation in patterne materials," Nature Mater. **1**, 95-98 (2002).
13. R. Morandotti, H. S. Eisenberg, Y. Silberberg, M. Sorel, and J. S. Aitchison, "Self-focusing and defocusing in waveguide arrays," Phys. Rev. Lett. **86**, 3296-3299 (2001).

#9456 - $15.00 USD Received 10 November 2005; revised 5 December 2005; accepted 7 December 2005

14. T. Pertsch, T. Zentgraf, U. Peschel, A. Brauer and F Lederer, "Anomalous refraction and diffraction in discrete optical systems," Phys. Rev. Lett. **88**, 093901 (2002).
15. H. A. Haus and L. Molter-Orr, "Coupled multiple waveguide systems," IEEE J. Quantum Electron. **QE-19**, 840-844 (1983).

1. Introduction

The size of light beam in conventional dielectric waveguides is around half the light wavelength due to the diffraction. As an evanescent wave excited on the interface between metals and dielectrics, surface plasmon polaritons (SPPs) can localize their energy in a nanoscale domain and circumvent the diffraction limit [1]. Based on this peculiar characteristic, Maier et al. have constructed a nanoscale SPP waveguide with linear chain of closely packed metal nanoparticles [2]. But SPPs propagating along this nanoparticle chain suffer from strong energy damping (3dB/100nm). Although metal gap waveguides composed of two parallel metal plates makes it possible to guide SPPs with rather low propagation loss in the nanoscale gap region [3], SPPs in one direction of the cross section is expanded to several hundreds of nanometers. Recently, by modulating phase-velocity (v_p) of SPPs on metal-dielectric interface with geometric width of guide region, Tanaka et al. proposed a three-dimensional (3D) nanoscale waveguides [4, 5]. Instead of varying the geometric parameters of metal-dielectric structures, the authors have demonstrated a kind of metal heterowaveguides (MHWGs) for nanofocusing [6] and beaming [7] of light as well as use as Bragg reflectors [8] by modulating v_p of SPPs through different metal and dielectric materials [6].

In this paper, instead of just constructing gap waveguides with two metal materials or with different guide width, respectively, for nanofocusing, beaming, mirrors or nanoguiding [4-8], we theoretically propose and numerically demonstrate a 3D MHWG constructed with two metal materials [6-8] and with different guide width [4, 5] simultaneously for the potential of MHWGs in the fields of nanophotonics such as nanosensing, nanolithography, array imaging, and controlling of the flow of light etc by using the finite-difference time-domain (FDTD) method [9].

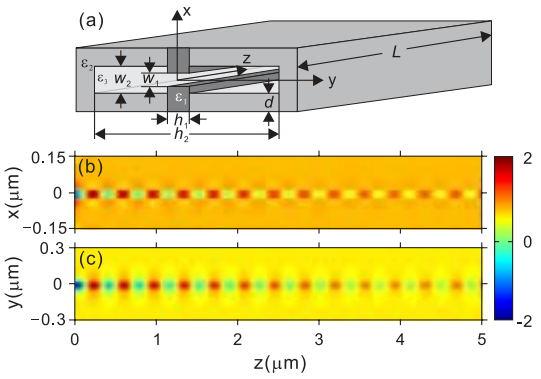

Fig. 1. (a) Scheme of the MHWG structure. w_1 and h_1 denote the width and height of Ag (with the dielectric constant of ε_1) guide and w_2 and h_2 is that of Al (ε_2) guides. (b) and (c) illustrate E_x distribution in x-z plane and y-z plane, respectively.

2. MHWG structures and propagation properties

The MHWGs we considered in this paper are constructed by inlaying a rectangular Ag waveguide into the centric part of an Al waveguide [Fig. 1(a)]. The geometric parameters such as the

#9456 - $15.00 USD Received 10 November 2005; revised 5 December 2005; accepted 7 December 2005

length of waveguide L (=5μm, fixed), the thickness of metal wall d (=85nm, fixed), the width and height of Ag guide ($w_1$and h_1 in x and y directions, respectively) and that of Al guide (w_2 and h_2) are all given in the figure. In our FDTD simulations, the spatial and temporal steps are $\Delta x=\Delta y=\Delta z=5$nm and $\Delta t=\Delta x/2c$, respectively, where c is light velocity in air. The dielectric constants of Ag and Al are given as ε_1=-10.55+j0.84 and ε_2=-42.13+j11.96, respectively, at incident wavelength λ=539.1nm [10], and the medium in the guide region is air (ε_3=1).

The guided modes in the MHGs are SPPs that can be excited by a TM-polarized incident wave (electric field parallel to x direction) at the metal surfaces and prefer to travel in the Ag guide region because in there SPPs are with lower v_p [6]. To intensively reduce the lateral dimension of SPPs in MHWGs, a feasible way is to enlarge the difference of v_p of SPPs in Ag and Al waveguides [6]. This can be realized by increasing the width difference of both waveguides, i.e., by narrowing (widening) the width of Ag (Al) waveguide. However, a narrow guide will produce strong propagation loss of SPPs [6] due to the increased SPP power penetrating into metals. To get a reasonable balance between the beam size and propagation loss of SPPs, one has to properly select the width arrangement of Ag and Al waveguides. Figure 1(b) and 1(c) show the E_x distributions in x-z and y-z plane, respectively, as a TM-polarized Gaussian wave excited SPPs pass through the MHWG. Where the widths of Ag and Al guides are w_1=35nm and w_2 = 85nm, respectively, and h_1=35nm and h_2=405nm. One can see that SPPs are mostly confined in the centric region of the MHWG. The propagation constant $\beta(=\beta_r+j\beta_i)$ can be achieved from the field distribution of E_x [4]. The calculated value of β_r is $1.46k_0$ ($k_0=2\pi/\lambda$)and that of β_i is dependent on the propagation loss of SPPs in the MHWG.

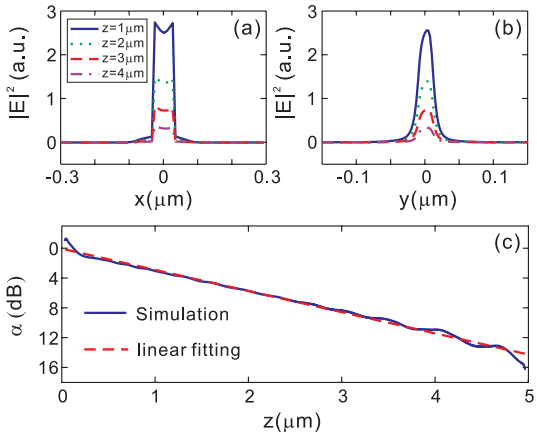

Fig. 2. $|E|^2$ profiles along (a) x direction at y=0 and (b) y direction at x=0 in x-y plane for different propagation distance. (c) Propagation loss as a function of the propagation distance.

Figures 2(a) and 2(b) depict the $|E|^2$ profiles along x direction at y=0 and y direction at x=0, respectively, for different propagation lengths (z direction). The full width at half maximum (FWHM) of $|E|^2$ is 35nm$\times$50nm at z=1μm, much narrower than the diameter of incident beam (200nm). The dependance of propagation loss of SPPs in the MHWG [defined as $\alpha=-10lg(S_z/S_0)$, S_z and S_0 present the Poynting vectors of SPPs at z and that of input wave, respectively] on the propagation distance is shown in Fig. 2(c). From the figure, we can get the average propagation loss of SPPs in the waveguide by linear fitting of the simulated values [11] and the result is about 2.84dB/μm. When changing the widths of Ag and Al guides, we get the cross section and propagation loss of SPPs in the waveguides as shown in Table 1. From the table, one sees that the cross section of SPPs is decreased and the propagation loss is reduced

#9456 - $15.00 USD Received 10 November 2005; revised 5 December 2005; accepted 7 December 2005

Table 1. Cross section and propagation loss of SPPs in the MHWGs for different w_1 and w_2.

w_1 (nm)	w_2 (nm)	FWHM in x direction (nm)	FWHM in y direction (nm)	Propagation loss (dB/μm)
15	15	15	115	9.05
15	35	15	45	6.46
15	55	15	45	4.70
25	25	25	170	6.46
25	35	25	50	5.27
25	55	25	45	4.27
25	85	25	45	2.94
35	85	35	50	2.84
55	85	55	65	2.77

as increased w_2 and fixed w_1. When w_2 is fixed, bigger w_1 results in the lager cross section of SPPs but smaller propagation loss. It is because that the cross section can be decreased by increasing the difference of v_p of SPPs in the waveguide and propagation loss can be reduced by increasing the widths of Ag or Al guide [6]. If there is no Al guide, however, the confinement of SPPs is vanished. To retain the confinement of SPPs, the geometric parameters of the Ag guide should be adjusted [4, 5]. The removal of Al guide makes against to achieve small cross section and small propagation loss of SPPs simultaneously.

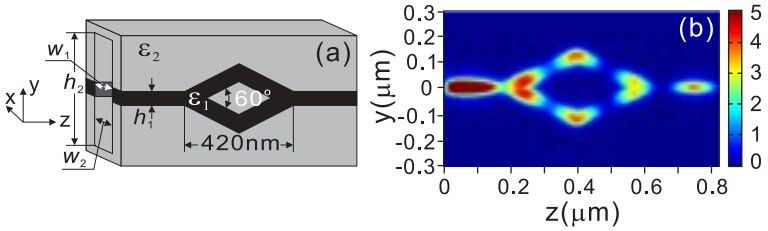

Fig. 3. (a) Scheme of the M-Z interferometer and (b) $|E|^2$ distributions in y-z plane at x=0 as SPPs passing through the interferometer.

3. Sensing property of MHWGs constructed Mach-Zehnder interferometer

To check the potential of such SPP waveguides in nanosensing, we design a nanoscale 3D Mach-Zehnder (M-Z) interferometer, a typical device in integrated optical circuits. Where, instead of inlaying a straight Ag waveguide in the center part of the Al waveguide as shown in Fig. 1(b), a shaped Ag waveguide is inlaid in place resulting in the formation of a 3D interferometer [Fig. 3(a)], where w_1=35nm, w_2=85nm, h_1=35nm and h_2=405nm, respectively. Figure 3(b) illustrates the $|E|^2$ distribution of SPPs in the interferometer structure. It clearly displays the split of SPPs evenly into two arms of the interferometer waveguide and then the recombination of the split SPPs in the output part. The totally about 30% of incident light energy can be transported to the output guide. The loss is due mainly to the scattering of SPPs in the junctions of waveguides. Taking advantage of the propagation properties of SPPs in the structure, nanoscale sensors can be realized. For example, when a sample is injected into one arm of the interferometer, the output signal will be modulated by the sample and the physical and chemical dynamics taking place in the sample can be analyzed in a nanoscale domain. In

#9456 - $15.00 USD Received 10 November 2005; revised 5 December 2005; accepted 7 December 2005

contrast to conventional interferometers [12], the nanoscale structures provide a way to greatly increase the detection sensitivity with relative small content of the samples and hence making such sensing as nanofluid detection possible. It should be pointed out that here we just present a model for nanosensors. As has been discussed above that the energy loss in M-Z structure is due mainly to the scattering of SPPs in the junctions of waveguides. Therefore, longer arms could be assembled within the interferometer for providing higher detection sensitivity.

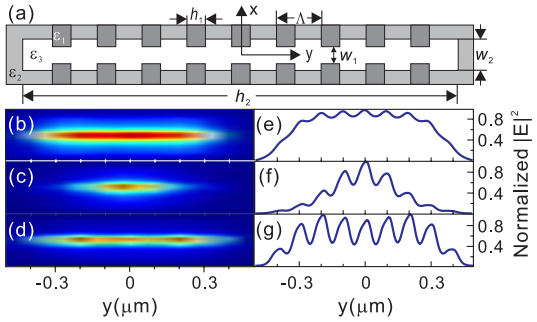

Fig. 4. (a) Cross section of the heterowaveguide array in x-y plane. (b)-(d) $|E|^2$ distributions of SPPs in a plane 25nm away from the output end of the structure and (e)-(g) the corresponding normalized intensity of $|E|^2$ profiles on a line parallel to x direction. w_2= (b) 35nm, (c) 55nm, and (d) 85nm while w_1=35nm.

4. DMHWs for array nanofocusing

On the other hand, much research interest is currently focused on the discrete optical systems (DOSs) due to their abnormal properties such as diffraction management and photonic Bloch oscillation and their potential in photonics [13, 14], but little attention is paid to the propagation behavior of electromagnetic fields in nanoscale DOSs. We have investigated SPPs propagation in one-dimensional metal gap waveguide arrays, and some interesting properties are deomnstrated [3]. However, such DOSs are constructed with a series of uniform metal gap waveguides and the cross section of SPPs in the DOSs is infinite in one dimension, which makes against the integration of optical devices. In the following part of the paper, we will study the propagation of SPPs in DMHWGs. Figure 4(a) shows the cross section of the structure, where the uniformly-spaced Ag waveguides with a period of Λ (=80nm), a width of w_1 (=35nm, fixed) and a height of h_1 (=35nm, fixed) is inlaid in the Al waveguide. The length of the guide region in y direction is given as h_2=805nm and that of the whole structure in z direction is 3μm. A TM-polarized plane wave is incident normally to one end of the structure (all MHWGs are excited) and the field intensity can be detected at the other open end. Figures 4(b)-4(d) illustrate the $|E|^2$ distributions in a x-y plane 25nm away from the output end of structure for the width of Al waveguide is given as w_2=35, 55, and 85nm, respectively. One sees clearly that there appears the nanospots in the near-field region, especially for the case w_2=85nm [Fig. 4(d)]. Figures 4(e)-4(g) show the corresponding normalized $|E|^2$ profiles at x=0 in the same plane. From the figures, we see that, as w_2 is smaller, the resolution of the maximum spots of $|E|^2$ is poor [Fig. 4(e)]. As w_2 is increased gradually, the spots become more discriminable [Figs. 4(f)-4(g)]. The cross section of each spot is about $60nm \times 65nm$ for w_2=85nm. Note that the field are converged in the center guides as w_2=55nm [Figs. 4(c) and 4(f)]. Figure 5 shows the E_x distributions in y-z plane at x=0 as w_2=35nm, 55 nm, and 85 nm, respectively. One sees that as w_2=35nm, there are two focuses observed in the array [Fig. 5(a)]. When w_2 is increased, the focuses shift away from the input plane [Figs. 5(b)-5(c)] and only one focus is observed as w_2=85nm due to the finite

#9456 - $15.00 USD Received 10 November 2005; revised 5 December 2005; accepted 7 December 2005

propagation distance [Fig. 5(c)]. These can be explained qualitatively with the coupled wave theory [15]. As the finite arrays and the boundary effect, coupled field in the waveguide arrays will be focused periodically and the period is dependent on the coupling length $L_c(=\pi/2C, C$ is the coupling coefficient of optical fields between adjacent guides), which describes the smallest length of energy exchange between adjacent waveguides. For smaller w_2, the cross section (along y direction) of light in individual waveguide is large resulting in strong coupling of SPPs between adjacent waveguides. Accordingly C is big and hence L_c is small. So the input energy will be focused in the center guides with a shorter propagation distance along z direction. As is shown in Figs. 4(c) and 4(f), the plane where we detected $|E|^2$ distribution is near to the second focus of light [Fig. 5(b)] in the array for w_2=55nm, therefore we see a converged $|E|^2$ distribution. In the other cases for w_1=35nm and 85nm, we see a almost uniformly $|E|^2$ distributions as the detecting plane is far away from the focused location in the arrays. From Fig. 4(d), we see that such heterowaveguide arrays may find interesting applications in the aspects as discrete array focusing, controlling the flow of electromagnetic fields in nanoscale domain, the fabrication of nanometric photonic devices, array sensing and etc.

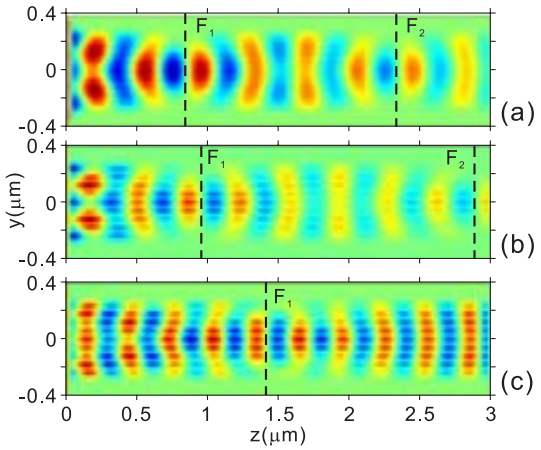

Fig. 5. E_x distributions in y-z plane for w_2= (a) 35nm, (b) 55nm and (c) 85nm. F_1 and F_2 denote the focus loacation in the DMHWGs.

5. Conclusion

In conclusion, by varying both the width and the dielectric properties of metal gap waveguides, we have theoretically proposed a 3D MHWG constructed with two metals. FDTD simulation reveals that light with a nanoscale cross section (35nm$\times$55nm) can propagate along a MHWG with a small loss (2.84dB/μm). With such MHWGs, we have designed a nanoscale M-Z interferometer for sensing with relative small content of the samples and hence making such sensing as nanofluid detection etc possible. A DMHWG system for array nanofocusing of light are also constructed and numerically demonstrated by FDTD simulation. A finite DMHWG array can focus an incident plane wave into nanospot array, implying potential applications of DMHWGs in near-field optics, nanolithography, array imaging, and controlling the flow of light etc.

Acknowledgments

We acknowledge financial supports from the Program for New Century Excellent Talents in University from Ministry of Education (NCET-04-0678) and the National Natural Science Foundation of China (grant 10574101).

#9456 - $15.00 USD Received 10 November 2005; revised 5 December 2005; accepted 7 December 2005